



ELSEVIER

Surface Science 311 (1994) 411–421

surface science

## Correlation functions in surface diffusion: the multiple-jump regime

R. Ferrando, R. Spadacini, G.E. Tommei \*, G. Caratti

*Dipartimento di Fisica dell'Università di Genova, Centro di Fisica delle Superfici e delle Basse Temperature / CNR, and  
unità INFN, via Dodecaneso 33, 16146 Genova, Italy*

(Received 14 December 1993; accepted for publication 27 January 1994)

### Abstract

Although the theories (transition state theory and jump diffusion) usually employed to describe surface diffusion cannot give information about the motion of adsorbed particles inside the potential wells, interesting results were obtained recently by MD simulations showing enhanced oscillations in the mean-square displacement before the linear behaviour in time is finally reached; at the same time evidence of long correlated jumps was found. In this paper the single-particle diffusion on surfaces is studied in the framework of the continuous Brownian model (Klein–Kramers equation). The Klein–Kramers dynamics is first analyzed by qualitative considerations about the dissipation integral, obtaining necessary and sufficient conditions on typical time scales in order to get different migration mechanisms. In particular, at high barriers, conditions are found for multiple jumps to be inhibited or to take place with small and considerable probability respectively. Then starting from the dynamic structure factor, the relevant correlation functions (velocity self-correlation spectrum and mean-square displacement) are evaluated, together with the jump probabilities, at the same potential barrier and friction of the MD calculations. At these values of the parameters diffusion proceeds, as expected, by a considerable fraction of multiple correlated jumps and many oscillations are found in the mean-square displacement in good agreement with MD results.

### 1. Introduction

Surface diffusion of adatoms is a very interesting problem from technological, experimental and theoretical viewpoints [1,2]. The atomic surface mobility controls the dynamics of many processes involving mass transport (growth of aggregates, chemical reactions, etc.) and is influenced by a great number of phenomena (structural and dy-

namical properties of surfaces, point as well as extended defects, chemical impurities etc.). Thus the microscopic study of well-defined crystal surfaces is of primary interest.

For a long time experimental efforts, mainly by field ion microscopy (FIM), were devoted to a systematic study of the single-particle diffusion coefficient  $D$  (or tracer diffusion coefficient [1]), on metal surfaces, in order to quantitatively determine the prefactor and the activation barrier in the Arrhenius law [1,3,4]. Recently great advances have been obtained employing high-resolution neutron [5] and atom [6] inelastic scattering

\* Corresponding author.

and elevated-temperature scanning tunneling microscopy (STM) [7]. These new techniques furnish the energy width of the dynamic structure factor [5,6] and a direct atomic-scale observation of adatom diffusion [7] on different kinds of surfaces (metals, molecular crystals, reconstructed surfaces).

The experimental results show the existence of a low-barrier unactivated regime at high surface temperature [5,8,9] and the important role of long jumps in several surfaces [7,10]. Long jumps have been also observed in molecular-dynamics simulations of CO adsorbed on Ni(111) [11]. Both these dynamical features (unactivated regimes, long jumps) can be explained in the framework of the Fokker–Planck equation (FPE) approach to single-particle diffusion in periodic media [9,12,13].

Except for hydrogen at low surface temperature, adatom diffusion is a classical transport problem. In the usual picture, the surface motion of a single classical adatom is described by a series of uncorrelated jumps between nearest-neighbour sites arranged in a lattice [3,4]. The adatom spends most of its time in moving around the positions of local stability, rarely hopping to adjacent sites with jump rate  $r_j$ ; the latter quantity is usually estimated by more or less refined versions of the transition state theory (TST) [4,14]. The single-jump model [15], although qualitatively correct in several cases of low-temperature diffusion, neglects the essential dynamical character of the diffusion. The adatom is coupled to the underlying crystal not only by a surface periodic potential (adiabatic potential) but also by a friction (generally a memory friction) [2,16]; in fact diffusion is intimately connected to fluctuations in the thermal bath.

The stochastic theory based on the FPE is able to describe different diffusion mechanisms. Quasi-continuous diffusion and hopping mechanisms (by single or multiple jumps) correspond to different ranges of the friction and of the potential barrier or, more physically, to different ratios between some typical time scales [13]. Long- and short-time dynamics can be quantitatively investigated by calculating the diffusion coefficient [9,17] and the relevant correlation functions [13] respec-

tively. In the hopping regime, the jump rate and the probability distribution of the jump lengths can be also extracted from the dynamical structure factor [18]. Moreover the FPE approach allows a detailed study of the dependence on the potential shape.

In the following we sketch the essential features of the stochastic theory and present some results in the low-friction, multiple-jump regime; the FPE description agrees well with the MD results for CO/Ni(111) [11].

## 2. Theory

Molecular-dynamics simulations [11,19] of surface diffusion of adsorbates have given interesting results about the short-time dynamics of the migrating particles showing several oscillations in the potential wells. Evidence of multiple correlated jumps was found in the same simulations [11], in experiments performed with FIM [10] and with atomic scattering [6], and more recently with the very sensitive STM technique [7]. We will show how these phenomena are recovered in a proper theory of surface diffusion.

Both from a theoretical and an experimental point of view, the quantity carrying the most complete information on the statistical properties of a system is the self-part of the dynamic structure factor  $S_s(q, \omega)$ , defined (in 1D notations) as the time Fourier transform of the characteristic function  $\Sigma_s(q, t)$ :

$$S_s(q, \omega) = \frac{1}{2\pi} \int_{-\infty}^{+\infty} e^{-i\omega t} \Sigma_s(q, t) dt, \quad (1)$$

where

$$\Sigma_s(q, t) = \langle \exp[iq(x(t) - x(0))] \rangle. \quad (2)$$

The brackets stand for the statistical average and  $x(t)$  and  $x(0)$  refer to the same particle;  $\hbar q$  and  $\hbar\omega$  are the momentum transfer and the energy loss respectively.

The derivatives of  $\Sigma_s$  with respects to  $q$ , evaluated in  $q = 0$ , give the moments of the displacements distribution (even moments only differing from zero) and all the self-correlation functions, as well as the transport coefficients, can be de-

duced from  $S_s$ , via the Green–Kubo relations [20], by doing suitable limits.

Let us briefly recall some of these fundamental relationships. The velocity self-correlation function  $Z(t)$  is defined as

$$Z(t) = \langle v(t)v(0) \rangle, \quad (3)$$

with a spectrum  $Z(\omega)$  given by the time Fourier transform

$$Z(\omega) = \frac{1}{2\pi} \int_{-\infty}^{+\infty} dt e^{-i\omega t} Z(t). \quad (4)$$

$Z(\omega)$  can be obtained from the dynamic structure factor [20],

$$Z(\omega) = \omega^2 \lim_{q \rightarrow 0} \frac{S_s(q, \omega)}{q^2}, \quad (5)$$

and its low-frequency limit is related to the tracer diffusion coefficient by

$$D = \pi \lim_{\omega \rightarrow 0} Z(\omega). \quad (6)$$

The mean-square displacement,  $w(t) = \langle [x(t) - x(0)]^2 \rangle$ , is deduced from the characteristic function  $\Sigma_s$  as

$$w(t) = -\frac{\partial^2}{\partial q^2} \Sigma_s(q, t) \big|_{q=0}. \quad (7)$$

Obviously, relationships may be found between  $w(t)$  and  $S_s$ ; one which has been used by us, for practical purposes, is the following:

$$w(t) = 4 \int_0^{+\infty} d\omega [1 - \cos(\omega t)] \lim_{q \rightarrow 0} \frac{S_s(q, \omega)}{q^2}. \quad (8)$$

As pointed out in the introduction, a method for evaluating  $S_s$  is of primary importance if surface migration processes of tagged particles are to be investigated in detail.

In the jump regime (high potential barriers) the dynamic structure factor can be calculated with discrete models (lattice gas models) [1,15,21]. However, interesting evidence of migration processes which cannot be described in the framework of jump models was found at high surface temperature [5]. Furthermore, and more important in the context of this paper, discrete models cannot look deeply inside the intra-well dynamics: rather they can only explore the inter-wells

migration mechanisms. The behaviour of the self-correlation functions  $Z(t)$  and  $w(t)$  as a function of time is clearly determined by both types of dynamics, the inter-wells and intra-well motions. While some quantities, such as the diffusion coefficient, are related to asymptotic behaviours in time, the motion inside a potential well can be explored in detail only looking also at short times and explicitly considering the presence of structured potential wells.

Continuous models must be employed for this purpose, and some kind of transport equation is needed to evaluate the average in Eq. (2). The Brownian motion model, briefly illustrated in the following, can give a complete treatment of the diffusive processes of a particle. In fact it can describe with continuity quasi-continuous regimes at low barriers as well as jump regimes, multiple correlated jumps included, at higher potentials. An extended description of the theory and of the main results attained, in every regime, for  $S_s$  and its full width at half maximum, for the diffusion coefficient and for the correlation functions is given elsewhere [9,13].

Here, after giving the essential features of the theory, we discuss in much more detail with respect to Ref. [13] the conditions required for multiple jumps being activated; furthermore new results in the multiple-jump regime and in the same conditions of Ref. [11] are presented.

Besides  $Z(\omega)$  and  $w(t)$ , also the probability of multiple correlated jumps is evaluated from  $S_s$  as [18]:

$$P_n = -\frac{a}{\pi r_j} \int_0^{\pi/a} \Delta\omega(q) \cos(naq) dq. \quad (9)$$

In Eq. (9)  $P_n$  is the probability of a jump of length  $na$  ( $a$  lattice spacing),  $\Delta\omega(q)$  is the full width at half maximum of the quasi-elastic peak of  $S_s$  and  $r_j$  is the total jump rate given by

$$r_j = \frac{a}{2\pi} \int_0^{\pi/a} \Delta\omega(q) dq. \quad (10)$$

### 2.1. The model

Let us now illustrate how the average in Eq. (2) can be calculated. The starting point is the

well-known stochastic equation, due to Langevin [22], for the motion of one Brownian particle in an external field,

$$m \frac{dv}{dt} = -m\eta v + m\Gamma(t) + F(x), \quad (11)$$

where  $-m\eta v$  and  $F(x)$  are the deterministic forces (damping and external force respectively) acting on the migrating particle. If the stochastic fluctuating force,  $\Gamma(t)$ , is assumed to be Gaussian, delta-correlated (white noise) and with zero average, an equivalent differential equation, of the Fokker–Planck type, may be written for the distribution function  $f(x, v, t)$  in the one-particle phase space [22],

$$\frac{\partial f}{\partial t} = -v \frac{\partial f}{\partial x} - \frac{F(x)}{m} \frac{\partial f}{\partial v} + \eta \frac{\partial}{\partial v} \left( v f + \frac{k_B T}{m} \frac{\partial f}{\partial v} \right), \quad (12)$$

where  $T$  is the temperature of the thermal bath. We will refer to this equation, following Risken's nomenclature [22], as to the Klein–Kramers equation (KKE).

The above-mentioned assumptions on  $\Gamma(t)$  are justified if both velocity and position of the migrating particle are varying on a slower time scale with respect to the correlation time of the fluctuations.

As for surface diffusion, the external force  $F(x)$  is due to the surface lattice, hence it is periodic and derivable from a potential i.e.  $F(x) = -\nabla U(x)$ . This point deserves some clarification. The interaction of the particle with the background is divided into two parts: a static one, giving rise to an adiabatic periodic potential (really a free energy, and therefore temperature-dependent), and a dynamic one here simulated by a friction force and by a purely stochastic force with white noise spectrum. The adparticle couples to the electronic excitations as well as to the lattice vibrations; as for the first coupling, the assumptions underlying the KKE are valid due to the small electron mass with respect to the mass of the adsorbed particle. The time scale separation is more cumbersome in the second case and, in general, non-Markovian effects, such as memory functions, should be included. Really, Wahn-

ström [16] rigorously demonstrated that the restrictive assumptions behind the KKE are fully satisfied, for a single adsorbate, if a periodic, position dependent, friction coefficient  $\eta(x)$  is considered and if the mass of the adsorbate is not less than the mass of the substrate atoms. However, also with a homogeneous friction and with a less favorable mass ratio we obtained very good results [8,12] in comparing our theory with experiments.

It must also be remarked that the 1D treatment, here presented, is valid for decoupled surface potentials; in fact, in this case, the 2D problem can be factorized into two independent 1D problems. Solutions of the KKE in two coupled dimensions have been recently obtained by the authors [23].

If the KKE is solved, the characteristic function (2) is found as

$$\begin{aligned} \Sigma_s(q, t) &= \langle \exp[iq(x(t) - x(0))] \rangle \\ &= \int_{-a/2}^{a/2} dx_0 \int_{-\infty}^{\infty} dv_0 \int_{-\infty}^{\infty} dx \int_{-\infty}^{\infty} dv \\ &\quad \times \exp[iq(x - x_0)] P_{st}(x_0, v_0) \\ &\quad \times P_c(x, v, t/x_0, v_0, 0). \end{aligned} \quad (13)$$

$P_{st}$  is the stationary probability given by the Boltzmann distribution and normalized to one particle per cell. The conditional probability  $P_c(x, v, t/x_0, v_0, 0)$  (i.e. the probability of having the particle in  $x$  and  $v$  at time  $t$  if it was in  $x_0$  and  $v_0$  at time 0) is the Green function of the KKE and is then obtained solving Eq. (12) with initial  $\delta$ -condition in the variables  $x$  and  $v$ .

The solution of the KKE depends on some parameters, those in the models describing the friction  $\eta(x)$  and the potential  $U(x)$ . In the simplest case (homogeneous damping and symmetric cosine potential), two parameters only are involved: the friction  $\eta$  and the strength of the potential amplitude with respect to  $k_B T$ . Very different migration mechanisms going from quasi-continuous to activated diffusion and, in the latter case, from single to multiple jumps, are described by the KKE depending on the values of the parameters [13].

## 2.2. The solution of the KKE

The KKE cannot be analytically solved in every regime, i.e. at every friction and at every value of the potential barrier. A numerical method of solution, the matrix continued fraction method (MCFM), has been developed by Risken [22,24]; the method, extended to the very general case of a position-dependent friction, has been already explained elsewhere [13] with much detail; the procedure is rather heavy and tedious, so here only the final result for  $S_s$  is recalled. Considering a periodic potential of lattice spacing  $a$ , the elementary cell goes from  $x = -a/2$  to  $x = a/2$ , while the first Brillouin zone in reciprocal space goes from  $q = -\pi/a$  to  $q = \pi/a$ . Defining the dimensionless friction  $\gamma$ ,

$$\gamma = \frac{a}{2\pi} \sqrt{\frac{m}{k_B T}} \eta, \quad (14)$$

the result for the dynamic structure factor is

$$S_s(q, \omega) = 2N \Re \left\{ \sum_{p,l=-\infty}^{\infty} \tilde{G}_{00}^{pl}(k, i\omega) M_{p-r} M_{l-r}^* \right\}, \quad (15)$$

where  $q = (2\pi/a)(k+r)$ , with  $-\frac{1}{2} < k \leq \frac{1}{2}$  and  $r$  integer. In Eq. (15)  $N$  is a normalization factor, the  $M_r$  are some coefficients depending on the potential and  $\tilde{G}_{00}$  is expressed as a continuous fraction of some matrices depending on the potential and on the friction. In writing Eq. (15) the same notations of Ref. [13] have been used.

Eq. (15) can now be numerically solved without too much effort, for a wide range of the parameters; the matrix continued fraction must be truncated at a certain number of iterations and matrices of finite size must be used. Problems in the computing time needed to get a good convergence can arise only at really extreme values of the parameters involved. The solution given here, being valid for every periodic potential shape and friction, is quite general. Once  $S_s$  has been calculated, the correlation functions are deduced from Eqs. (5) and (8). Before giving the results obtained for the multiple-jump regime, we discuss the different diffusive mechanisms described by the KKE.

## 2.3. Characteristic times and diffusive regimes

A qualitative discussion on the KKE dynamics may be done, without explicitly solving the equation, on the basis of the characteristic time scales contained in the KKE. As in this paper the interest is focused on the multiple-jump regime, a more detailed analysis is required with respect to Ref. [13]. For simplicity a position independent friction  $\eta$  is considered. In this case four times govern the solution of Eq. (12):

- (1) The velocity correlation time  $\tau_v \approx \eta^{-1}$ .
- (2) The small oscillation period  $\tau_{osc}$  at the well bottom.
- (3) The imaginary period  $\tau_{im}$ , due to the inverse curvature at the barrier top.
- (4) The time  $\tau_{th}$  taken by the particle to cross over a lattice spacing with mean thermal velocity  $v_{th} = \sqrt{k_B T/m}$ .

To simplify the discussion, we will take into account only three times, putting  $\tau_{osc} = |\tau_{im}|$  as in symmetric potentials.

In order to discriminate between the high- and low-friction regimes, the mean energy dissipated on a lattice spacing  $a$  must be considered:

$$\Delta E_c = \int_{-a/2}^{a/2} m\eta v(x) dx. \quad (16)$$

Putting the potential maxima at  $U=0$  and the minima at  $U=-E_b=-2A$ , where  $A$  is the potential amplitude (see Fig. 1), the initial total energy of a particle starting from  $x = -a/2$  with thermal velocity  $v_0$  will be written as  $E_0 = \frac{1}{2}mv_0^2 = \frac{1}{2}k_B T$ . With the approximation

$$v(x) \approx \sqrt{\frac{2}{m} [E_0 - U(x)]}, \quad (17)$$

the energy dissipated on a cell may be estimated as

$$\Delta E_c \approx \eta \int_{-a/2}^{a/2} \sqrt{m[k_B T - 2U(x)]} dx \quad (18)$$

and the low-friction regime is defined by the condition

$$\Delta E_c \ll k_B T. \quad (19)$$

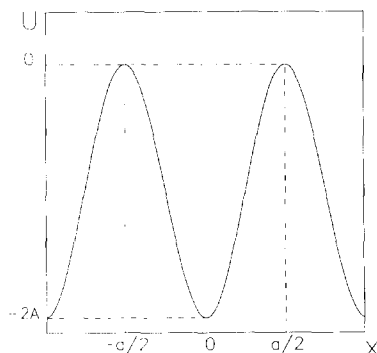


Fig. 1. Schematic sketch of the generic periodic potential  $U(x)$  assumed in the text for qualitative considerations about the dissipation integral. The potential maxima are put at  $U=0$  and the minima at  $U=-E_b=-2A$ ; the elementary cell goes from  $x=-a/2$  to  $x=a/2$ , where potential maxima are located.

As  $-2U(x) > 0$ , the inequality (19) necessarily implies that

$$\eta \int_{-a/2}^{a/2} \sqrt{mk_B T} \, dx \ll k_B T \quad (20)$$

i.e.

$$\tau_v \gg \tau_{th}. \quad (21)$$

The latter condition is also sufficient if  $|U(x)|$  is never much larger than  $k_B T$ .

On the contrary if  $E_b \gg k_B T$ , Eq. (19) can be rewritten as

$$\eta I(E_b) = \eta \int_{-a/2}^{a/2} \sqrt{-2mU(x)} \, dx \ll k_B T, \quad (22)$$

$I(E_b)$  is one half of the reduced action [25] at the barrier energy ( $E=0$ ); for deep wells  $I(E_b) \approx E_b \tau_{osc}$  [26] and therefore condition (19) becomes

$$\frac{\tau_{osc}}{\tau_v} \ll \frac{k_B T}{E_b}. \quad (23)$$

Eqs. (21) and (23) specify the necessary and sufficient conditions for being in the low-friction regime at high barriers.

Obviously, if  $E_b \gg k_B T$ , the relationship (23) leads to

$$\tau_v \gg \tau_{osc}, \quad (24)$$

the latter relationship, together with (21), gives a couple of necessary (not sufficient) conditions for the low-friction regime at high barriers.

As for the high-friction regime, where the Smoluchowski equation is a good approximation of the KKE [27,28], it will be recovered under opposite conditions:

$$\tau_v \ll \tau_{th}, \quad \tau_v \ll \tau_{osc}. \quad (25)$$

In fact the high-friction limit of the KKE is an equation in configuration space; the velocity immediately thermalizes and then its correlation time must be the shortest one in the problem.

Both in the low- and in the high-friction regime, the diffusion can be quasi-continuous or it can proceed by jumps as in discrete models. The jumping condition requires that the particle spends most of its time in small amplitude motions around the potential minima; this happens when the curvature at the well bottom is sufficiently high, that is when

$$\tau_{osc} \ll \tau_{th}. \quad (26)$$

For sinusoidal potentials this is equivalent to say that  $E_b$  is considerably larger than  $k_B T$ .

For multiple jumps being activated with appreciable probability, the velocity must be self-correlated for a long time, hence low friction is required. So the necessary and sufficient conditions are given by (21) and (23).

As an example, in order to summarize the matter, we consider a sinusoidal potential

$$U(x) = -A[1 + \cos(2\pi x/a)], \quad (27)$$

and define the dimensionless quantity

$$g = A/2k_B T; \quad (28)$$

the characteristic times are then

$$\tau_{osc} = a\sqrt{m/A}, \quad \tau_v = 1/\eta, \quad \tau_{th} = a\sqrt{m/k_B T}. \quad (29)$$

The conditions determining the different diffusive mechanisms can be rewritten by means of  $\gamma$  and  $g$ .

(a) At low barriers ( $g < 1$ ) the low-friction regime is identified by

$$\tau_v \gg \tau_{th} \leftrightarrow \gamma \ll 1. \quad (30)$$

(b) At high barriers ( $g > 1$ ) the low-friction regime is identified by relationship (30) and by

$$\frac{\tau_{\text{osc}}}{\tau_v} \ll \frac{k_B T}{E_b} \leftrightarrow \gamma \ll \frac{1}{\sqrt{g}}. \quad (31)$$

(c) The condition for the jump regime is

$$\tau_{\text{osc}} \ll \tau_{\text{th}} \leftrightarrow g > 1. \quad (32)$$

(d) Long jumps are activated when relationships (30) and (31) are both satisfied. Condition (32) is automatically verified.

(e) The Smoluchowski equation can be safely applied if

$$\begin{aligned} \tau_v &\ll \tau_{\text{th}} \leftrightarrow \gamma \gg 1, \\ \tau_v &\ll \tau_{\text{osc}} \leftrightarrow \gamma \gg \sqrt{g}. \end{aligned} \quad (33)$$

In case (e) at high barriers single jumps only are activated; in fact, multiple jumps are inhibited

because, after jumping one lattice spacing, the particle is immediately trapped into the nearest well due to the very short correlation time of the velocity.

The equivalence between the first and the second columns in the previous inequalities deserves some comment; the relationships in the second column are written in terms of the essential dependence on  $\gamma$  and  $g$  without numerical factors; as a consequence, these conditions result to be less restrictive with respect to the corresponding ones in the first column. In effect the qualitative arguments above developed are rather drastic; in particular, Eqs. (23) and (26) are to be intended in the sense that the first member must be at most of the same magnitude of the second one. We numerically verified that realistic conditions are really furnished in the second column.

From above, the plane of the parameters  $\gamma$  and  $g$  is divided into five regions, each corresponding to different migration mechanisms (Fig. 2). The lower and upper curve dividing regions (2), (3) and (4) are  $\gamma = 1/\sqrt{g}$  and  $\gamma = \sqrt{g}$  respectively. The division is rather schematic and typical characteristics of the zones are fully realized far from the boundaries.

Summarizing, in Fig. 2:

- zone 1: low friction, quasi-continuous diffusion;
- zone 2: low friction, jump diffusion, considerable probability of multiple jumps;
- zone 3: intermediate friction, jump diffusion, small probability of multiple jumps;
- zone 4: high friction, jump diffusion, single jumps only;
- zone 5: high friction, quasi-continuous diffusion.

Fig. 2 has been obtained discussing a sinusoidal potential (three times, two parameters only); however, the essential features of this qualitative discussion on the diffusion mechanisms are not changed if more parameters are to be considered. The qualitative predictions here presented are fully confirmed by numerical results [13]. The proper quantity to immediately distinguish between quasi-free and jump diffusion and, in the latter case, between single and multiple jumps, is the full width at half maximum of the

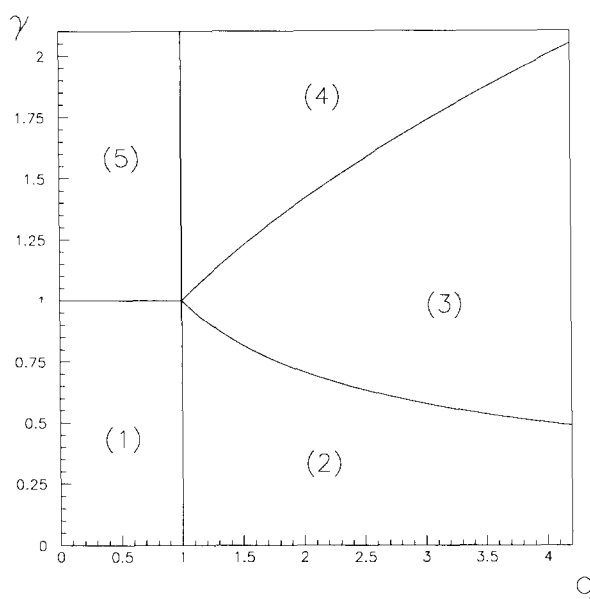


Fig. 2. Different diffusive regimes as located in the plane ( $g, \gamma$ ), for the case of a cosine potential, by roughly calculating the dissipation integral on the basis of the typical times involved in the Klein–Kramers dynamics. The lower and upper curves separating zones (4), (3) and (2) are  $\gamma = \sqrt{g}$  and  $\gamma = 1/\sqrt{g}$  respectively. In regions (1) (low friction) and (5) (high friction) quasi-continuous diffusion takes place while in the other regions diffusion proceeds by jumps, long jumps being strictly forbidden in region (4). Multiple correlated jumps occur with large probability only in zone (2).

quasi-elastic peak of  $S_s$ . For this purpose, the reader is referred to paper [13].

In the following the attention is focused on solutions of the KKE in region 2.

### 3. Results in the multiple-jump regime

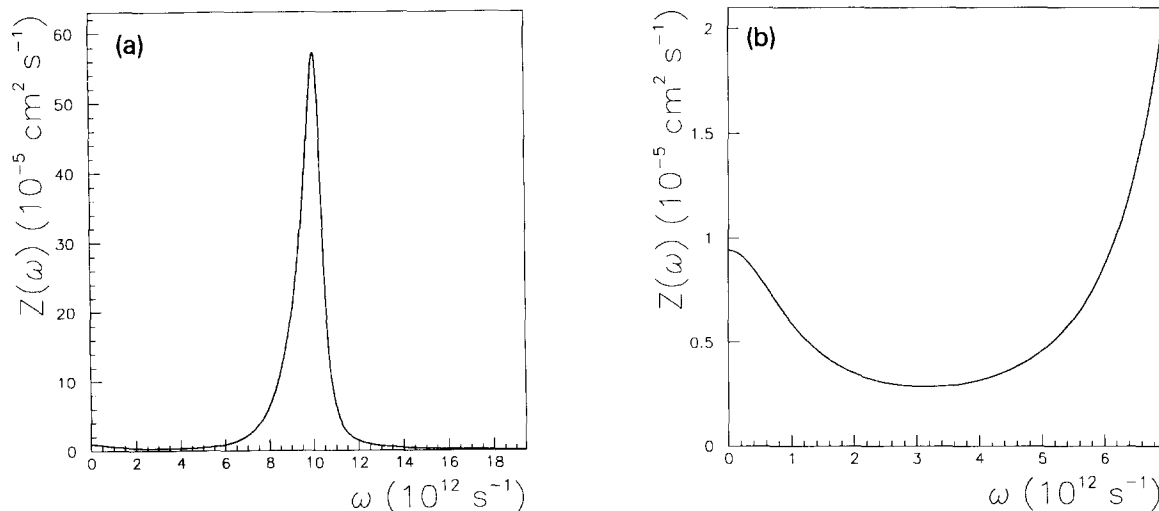
From the dynamic structure factor, numerically evaluated by the MCFM, the velocity self-correlation spectrum  $Z(\omega)$  and the mean-square displacement  $w(t)$  are calculated from Eqs. (5) and (8).

As discussed in Ref. [13], in the high-friction regime, the dynamic structure factor behaves, at fixed  $q$ , as a monotonically decreasing function of  $\omega$ . This is no longer true in the low-friction regime where, at sufficiently high barriers,  $S_s$  always presents, at every  $q$ , an inelastic peak near  $\omega_{\text{osc}} = 2\pi/\tau_{\text{osc}}$ , the frequency of the small amplitude oscillations in the wells. These resonances do not appear in the high-friction regime because oscillations are immediately damped due to the  $\delta$ -like velocity correlation. Low friction and high barriers are realized in region 2 of Fig. 2, where diffusion proceeds by jumps with a considerable

probability of long jumps. Such a behaviour of  $S_s$  corresponds to interesting correlation functions.

With respect to the well dynamics, the correlation functions are the most sensitive quantities; in fact, even at high friction where  $S_s$  do not show any other peak than the quasi-elastic one,  $Z(\omega)$  presents broadened maxima at about  $\omega_{\text{osc}}$ , more pronounced at higher  $g$ . Coherent oscillations in the wells are inhibited but  $Z(t)$  reveals even small parts of oscillations performed by the particle with unthermalized velocity.

Results for  $Z(\omega)$  and  $w(t)$  are presented here in the low-friction regime. The parameters determining the solution of the KKE have been deduced from data given in Ref. [11], where the diffusion of CO on Ni(111) is studied by MD simulations finding considerable quantities of long jumps. The surface temperature and the lattice spacing are  $T = 200$  K and  $a = 2.48$  Å respectively, giving then a thermal time  $\tau_{\text{th}} = 1.02$  ps; the authors estimate a potential barrier of  $6k_{\text{B}}T$ , corresponding to  $g = 1.5$ , and a velocity correlation time  $\tau_v \approx 3$  ps, giving rise to a position-independent friction  $\eta \approx 33 \times 10^{10} \text{ s}^{-1}$ ; then, from Eq. (14), the corresponding dimensionless quantity is  $\gamma = 0.05$ . The results in Ref. [11] show that



Figs. 3. The velocity correlation spectrum  $Z(\omega)$  obtained numerically solving the Klein-Kramers equation, for a cosine potential, by the matrix continued fraction method, at friction  $\gamma = 0.05$  and potential strength  $g = 1.5$  as in Ref. [11]. A very well-defined inelastic peak is shown in (a) at  $\omega_{\text{osc}} \approx 1 \times 10^{13} \text{ rad/s}$ , the small oscillation frequency at the well bottom. The behaviour of  $Z(\omega)$  at small  $\omega$  is enhanced in (b).



long jumps are mostly made along a straight line; then the 1D model here presented can be justified in order to qualitatively investigate the diffusion mechanism, as well as the choice of a simple cosine potential like that in Eq. (27). This choice gives  $\tau_{\text{osc}} = 0.59$  ps and  $\omega_{\text{osc}} = 2\pi/\tau_{\text{osc}} = 1.06 \times 10^{13}$  rad/s as from Eq. (29). The values of  $\gamma$  and  $g$  satisfy conditions (30), (31), (32) and are then fully placed in region 2 of the plane ( $g, \gamma$ ) where multiple-jump diffusion is expected. As for the first column in inequalities (30), (31) and (32), the conditions are verified only in the sense previously specified. The calculated  $S_s$  presents an inelastic peak near  $\omega_{\text{osc}}$  and the results for  $Z(\omega)$  and  $w(t)$  are shown in Figs. 3 and 4 respectively.

The velocity correlation spectrum in Fig. 3a shows a well-defined peak at  $\omega_{\text{osc}} \approx 1 \times 10^{13}$  rad/s; the behaviour of  $Z(\omega)$  at small  $\omega$  is enlarged in Fig. 3b; from the figure and from Eq. (6) the diffusion coefficient turns out to be  $D = 3 \times 10^{-5} \text{ cm}^2 \text{ s}^{-1}$ . This value very well agrees with the Arrhenius plot value in Ref. [11],  $D \approx 3.3 \times 10^{-5} \text{ cm}^2 \text{ s}^{-1}$ .

The mean-square displacement is plotted in Fig. 4 where many oscillations in the same potential well are shown with a period  $\tau_{\text{osc}} \approx 0.6$  ps. This is in full agreement with the previous behaviour of  $Z(\omega)$ . As the velocity correlation spec-

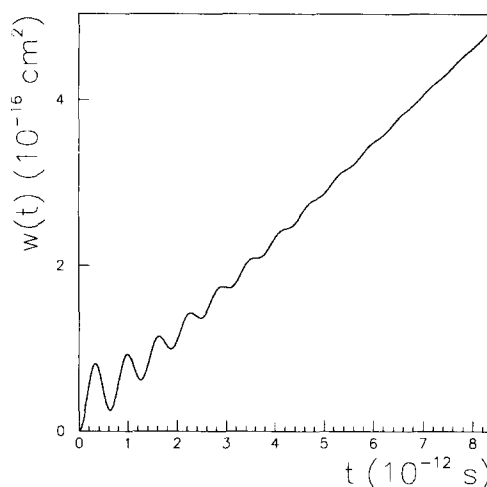
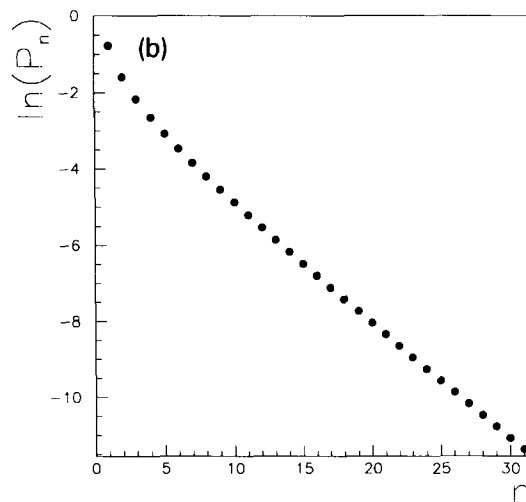
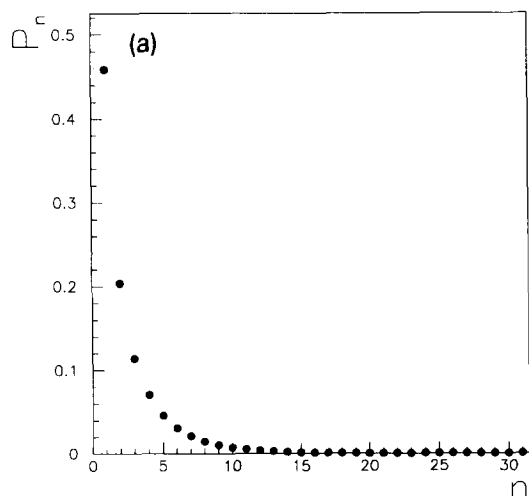


Fig. 4. The mean-square displacement  $w(t)$  in the same conditions of Fig. 3; at short times,  $w(t)$  oscillates about the linear trend due to the intra-well motion.

trum has a narrow peak the corresponding  $Z(t)$  will be nearly a damped cosine as in harmonic solids. Then, from the well-known relationship

$$Z(t) = \frac{1}{2} \frac{\partial^2}{\partial t^2} w(t), \quad (34)$$

oscillations are to be expected in  $w(t)$ . The calculated  $w(t)$  agrees well with the mean-square dis-



Figs. 5. (a) In the same conditions of Figs. 3 and 4, the probability  $P_n$  of correlated jumps of length  $na$  is drawn, clearly showing a large quantity of long jumps. (b) As in (a), but logarithmic scale is used to enhance the probability values at very large  $n$ .

placement of Ref. [11], nearly even quantitatively; of course the comparison between our time and space values and the corresponding ones in MD simulations must be made remembering that our model is 1D and the asymptotic behaviour of  $w(t)$  is then  $w(t) = 2Dt$  while in 2D it is  $w(t) = 4Dt$ .

The only relevant difference with MD simulations is in the oscillation period, being  $\tau_{\text{osc}} \approx 1.1$  ps in Dobbs and Doren work; the discrepancy is due to the cosine potential.

As shown by Eq. (9), at high barriers the jump probabilities can be calculated by the Fourier analysis of the quasi-elastic peak of  $S_s$ . The results, for the same values of  $\gamma$  and  $g$  previously used, are given in Fig. 5, clearly showing that multiple jumps play a relevant role as expected. It must be remarked that we define the probability  $P_n$  of a jump of  $n$  lattice spacings, as the probability that a particle, starting at thermal equilibrium from the cell 0, thermalizes again in the  $n$ th cell [18]. Our definition coincides with that of jump-diffusion theory, which is usually employed in the interpretation of the experimental data [10]. Really, Dobbs and Doren's definition, based on the number of dividing surfaces crossed, is different; however, in both cases, a considerable (and similar) proportion of long jumps is found.

#### 4. Conclusions

In this paper the surface diffusion of adsorbates has been studied, looking particularly at the multiple-jump regime, usually investigated employing discrete models. The continuous theory here presented, based on a Brownian model in the framework of the Klein–Kramers equation, can furnish complete information on the diffusive process by the calculation of the dynamic structure factor. The theory strictly holds for the diffusion of tagged particles and cannot then describe collective or chemical diffusion.

After giving the fundamental features of the theory and broad outlines of the numerical method of solution of the KKE, the Klein–Kramers dynamics has been investigated in much detail by qualitative arguments on the dissipation

integral; different migratory mechanisms are recovered according to the ratios between typical time scales. In the simple case of symmetric potential shapes, three characteristic times are involved, and necessary and sufficient conditions are established discriminating between quasi-free and jump diffusion and, in the latter case, between regimes where single jumps only are activated and regimes with a small or a considerable probability of multiple jumps. In the particular case of sinusoidal potential shapes, conditions on the time scales can be brought back to conditions on the friction  $\gamma$  and on  $g$ , the potential strength with respect to the thermal energy. In this simple case five different diffusive regimes have been located in the plane  $(g, \gamma)$  (Fig. 2); if  $g > 1$ , i.e. at high barriers, diffusion proceeds by jumps and two curves  $\gamma = \sqrt{g}$  and  $\gamma = 1/\sqrt{g}$  (high and very low friction respectively) precisely identify the single- or multiple-jump regimes.

The velocity self-correlation spectrum and the mean-square displacement, as well as the jump probabilities, have been then evaluated in region (2) of the plane  $(g, \gamma)$  where multiple jumps were expected by the previous considerations on the dissipation integral. The values of  $\gamma$  and  $g$  were chosen as in Ref. [11] where surface diffusion was studied by MD simulations, in conditions of high barriers and very low friction. Fig. 5a shows that the KKE assigns to single uncorrelated hops a probability of  $\sim 46\%$ , clearly indicating that diffusion proceeds by a considerable quantity of long jumps, in agreement with our qualitative discussion and with MD simulations. At the same time, interesting behaviours were found in the correlation functions where the short-time motion of adsorbates is revealed. The velocity correlation spectrum (Fig. 3a) has a well-defined peak due to the nearly harmonic motion at the bottom of the potential wells, and correspondingly many oscillations are found (Fig. 4) in the mean-square displacement before the asymptotic linear behaviour in time is reached, as obtained by Dobbs and Doren simulations. The theory has been numerically applied to a cosine potential but it could be also used for any potential shape.

From above and from previous results [8,9,12,13] the continuous theory here applied to in-

investigate the multiple-jump regime appears to be a good and very complete method to investigate both long- and short-time dynamics of particles diffusing on surfaces.

## References

- [1] R. Gomer, *Rep. Prog. Phys.* 53 (1990) 917.
- [2] T. Ala-Nissila and S.C. Ying, *Prog. Surf. Sci.* 39 (1992) 227.
- [3] G. Ehrlich and K. Stolt, *Ann. Rev. Phys. Chem.* 31 (1980) 603;  
T.T. Tsong, *Prog. Surf. Sci.* 10 (1980) 165.
- [4] V.P. Zhdanov, *Surf. Sci. Rep.* 12 (1991) 183.
- [5] M. Bienfait, J.P. Coulomb and J.P. Palmari, *Surf. Sci.* 182 (1987) 557; Erratum, *Surf. Sci.* 241 (1991) 454;  
M. Bienfait, J.M. Gay and H. Blank, *Surf. Sci.* 204 (1988) 331;  
M. Bienfait, P. Zeppenfeld, J.M. Gay and J.P. Palmari, *Surf. Sci.* 226 (1990) 327.
- [6] J.W.M. Frenken, B.J. Hinch, J.P. Toennies and Ch. Wöll, *Phys. Rev. B* 41 (1990) 938;  
B.J. Hinch, J.W.M. Frenken, G. Zhang and J.P. Toennies, *Surf. Sci.* 259 (1991) 288.
- [7] E. Ganz, S.K. Theiss, I. Hwang and J. Golovchenko, *Phys. Rev. Lett.* 68 (1992) 1567.
- [8] R. Ferrando, R. Spadacini and G.E. Tommei, *Surf. Sci.* 251/252 (1991) 773; *Surf. Sci.* 269/270 (1992) 184.
- [9] R. Ferrando, R. Spadacini and G.E. Tommei, *Surf. Sci.* 265 (1992) 273.
- [10] M. Lovisa and G. Ehrlich, *J. Phys. (Paris)* 50 (1989) C8-279;  
G. Ehrlich, *Surf. Sci.* 246 (1991) 1.
- [11] K.D. Dobbs and D.J. Doren, *J. Chem. Phys.* 97 (1992) 3722.
- [12] R. Ferrando, R. Spadacini and G.E. Tommei, *Phys. Rev. B* 45 (1992) 444.
- [13] R. Ferrando, R. Spadacini, G.E. Tommei and G. Caratti, *Physica A* 195 (1993) 506.
- [14] C. Wert and C. Zener, *Phys. Rev.* 76 (1949) 1169;  
G.H. Vineyard, *J. Phys. Chem. Solids* 3 (1957) 121.
- [15] C.T. Chudley and R.J. Elliott, *Proc. Phys. Soc. (London)* 77 (1961) 353.
- [16] G. Wahnström, *Surf. Sci.* 159 (1985) 311.
- [17] R. Ferrando, R. Spadacini and G.E. Tommei, *Surf. Sci.* 287/288 (1993) 866.
- [18] R. Ferrando, R. Spadacini and G.E. Tommei, *Phys. Rev. A* 46 (1992) R699; *Phys. Rev. E* 48 (1993) 2437.
- [19] H.K. McDowell and J.D. Doll, *J. Chem. Phys.* 78 (1983) 3219.
- [20] J.P. Hansen and I.R. McDonald, *Theory of Simple Liquids* (Academic Press, London, 1976);  
S.W. Lovesey, *Condensed Matter Physics-Dynamic Correlations* (Benjamin/Cummings, Menlo Park, CA, 1986).
- [21] M. Bée, *Quasielastic Neutron Scattering* (Hilger, Bristol, 1988).
- [22] H. Risken, *The Fokker–Planck Equation* (Springer, Berlin, 1989).
- [23] R. Ferrando, R. Spadacini, G.E. Tommei and G. Caratti, in preparation.
- [24] H. Risken and H.D. Vollmer, in: *Noise in Nonlinear Systems*, Vol. 1, Eds. F. Moss and P.V.E. McClintock (Cambridge Univ. Press, Cambridge, 1989).
- [25] L.D. Landau and E. Lifshitz, *Mécanique* (MIR, Moscow, 1966).
- [26] H.A. Kramers, *Physica* 7 (1940) 284.
- [27] S. Chandrasekhar, *Rev. Mod. Phys.* 15 (1943) 1.
- [28] J. Wilemski, *J. Stat. Phys.* 14 (1976) 153.